Extraction of Stripline Surface Roughness Using Cross-section Information and S-parameter Measurements

1st Ze Sun
EMC Laboratory
Missouri University of S&T
Rolla, USA
sunz1@umsystem.edu

2nd Jian Liu
Cadence Design Systems
San Jose, USA
jliu@cadence.com

3rd Xiaoyan Xiong
Cadence Design Systems
San Jose, USA
xiongx@cadence.com

4th Victor Khilkevich
EMC Laboratory
Missouri University of S&T
Rolla, USA
khilkevichv@mst.edu

5th DongHyun Kim
EMC Laboratory
Missouri University of S&T
Rolla, USA
dkim@mst.edu

6th Daryl Beetner
EMC Laboratory
Missouri University of S&T
Rolla, USA
daryl@mst.edu

2022 IEEE International Symposium on Electromagnetic Compatibility & Signal/Power Integrity (EMCSI) | 978-1-6654-0929-2/22/$31.00 ©2022 IEEE | DOI: 10.1109/EMCSI39492.2022.9889527

***Abstract*—To characterize additional conductor loss introduced by conductor surface roughness, various models have been proposed to describe the relationship between foil roughness levels and surface roughness correction factor. However, all these empirical or physical models require a PCB sample to be manufactured and analyzed in advance. The procedure requires dissecting the PCB and is time- and labor-consuming. To avoid such a process, a new surface roughness extraction process is proposed here. Only the measured S-parameter and nominal cross-sectional information of the board are needed to extract the roughness level of conductor foils. Besides, this method can also deal with boards having non-equal roughness on different conductor surfaces, which is common in the manufactured printed circuit boards (PCB). The roughness level on each surface can be extracted separately to accurately model their contribution to the total conductor loss. The presented method is validated by both simulation and measurement. A good correlation is achieved between extracted roughness level and the measured value from the microscope.**

***Index Terms*—Surface roughness, striplines, printed circuit board, signal integrity**

I. Introduction

To evaluate the signal integrity performance of high-speed channels, conductor loss needs to be characterized accurately. The skin effect formulas are widely used to calculate the conductor loss assuming a smooth conductor surface. However, roughness is intentionally created on the conductor surfaces to promote adhesion to the dielectric material in the PCB manufacture process [1] [2]. At frequencies of tens of gigahertz, ignoring the surface roughness of foils can lead to a significant underestimation of conductor loss [3].

To calculate the additional loss introduced by the rough surfaces, various approaches were proposed [4]- [7]. Even though the roughness-related formulas used in each method are not the same, the process they follow is similar. First, a micro-sectioned sample of PCB is produced and then photographed, depending on the desired resolution, either by an optical or scanning electron microscope (SEM). Next, the rough foil is modeled with simple geometric structures, like wedges, spheres, or semi-spheres. The size of the structure is determined by the profile of the conductor surface obtained in the first step. Finally, the additional loss introduced by the periodic structure is calculated analytically. The ratio between the conductor loss of rough and smooth cases is defined as the surface roughness correction factor K.

The main challenge of calculating correction factor K from conductor surface profile information is that a PCB sample needs to be manufactured and photographed in advance. This is time-consuming and requires optical or, in the case of ultra-smooth foils, which become more and more common, SEM equipment that is not available in many RF labs.

Besides, in the manufactured PCB boards, roughness on different conductor surfaces is not always the same. The sides attached to the core laminate are usually rougher to ensure a better adhesion, as presented in Fig. 1. In this case, assuming the same roughness level on all surfaces is not accurate anymore. Instead, different protrusion sizes should be assigned to each surface separately.

In this paper, a new surface roughness characterization method is proposed. Given the S-parameter measurement result and the cross-section geometry of the test board, the size of protrusions on different conductor surfaces can be determined separately. Compared with the optical or SEM imaging, the S-parameter measurement is much easier to perform, and test boards will not be damaged to make cross-sections. Thus, both time and money are saved in the extraction process.

This paper is organized as follows. First, in section II, the

additional loss introduced by the rough conductor surface is extracted from the measured S-parameter. Next, the roughness levels on each conductor surface are further reconstructed. Then, the proposed method is validated in section III by three examples, one uses measurement data of a fabricated PCB board, the other two use simulation result of the transmission line. Section IV concludes the paper.

II. Extraction of Additional Loss Introduced by Rough Surface From S-parameter

To determine the contribution of the conductors to the total loss (which is obtained directly from the transmission coefficient measurement), the dielectric loss contribution needs to be determined first [8] [9]. This is achieved by applying the loss tangent measurement method described in [10]. The method needs two strongly coupled stripline pairs of different lengths for accurate de-embedding (removing the reflections association with the cable-to-stripline or probe-to-stripline transitions [11]- [13]) and the loss tangent extraction.

The total attenuation factor α can be calculated from the de-embedded transmission coefficient S_{21} as:

$$\alpha = \frac{-\ln[|S_{21}|]}{l} \tag{1}$$

where l is the length of the transmission line after the de-embedding.

After determining the dielectric loss tangent, the dielectric contribution to the attenuation factor is calculated as:

$$\alpha_{diel} = \frac{1}{2} \cdot \tan\delta \cdot \omega \cdot \sqrt{LC} \tag{2}$$

where L and C are the per-unit-length (PUL) inductance and capacitance of the line (modal parameters for the differential pair are used as described in [10]), which are obtained through the 2-D simulation.

Then, the conductor loss factor is obtained as:

$$\alpha_{cond} = \alpha - \alpha_{diel} \tag{3}$$

For low loss transmission line, the conductor loss of the line can also be related to the PUL parameters as:

$$\alpha_{cond} \approx \frac{R}{2Z_0} \approx \frac{1}{2} R \sqrt{\frac{C}{L}} \tag{4}$$

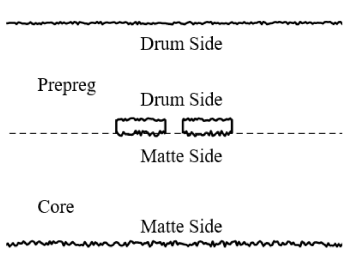

Fig. 1: The roughness on different surfaces of conductors is not the same.

where R is the PUL resistance of the line. Therefore, the PUL resistance of the rough line is:

$$R = 2\alpha_{cond}\sqrt{\frac{L}{C}} \tag{5}$$

As mentioned in the introduction, it is found that roughness on different surfaces of conductors is not the same in many PCB boards. Due to the manufacturing techniques used in the PCB fabrication, the matte side facing the core laminate is usually rougher than the drum side. To model this phenomenon, two sets of roughness settings in the 2-D solver need to be applied to different conductor boundaries. One set is applied to the drum side of the conductors (the bottom surface of the top ground, top and two side walls of trace), while the other set is applied to the matte side (the top surface of the bottom ground and the bottom surface of traces).

We propose to perform the estimation of the roughness parameters in the following algorithm:

1. A 2D cross-sectional model of the transmission line is created. The dielectric parameters and the PUL resistance of the rough conductors are determined from the measurement as discussed above.

2. Roughness models are created for the matte and drum surfaces of the conductors.

3. Parameters of the roughness models are iteratively optimized to minimize the error function reflecting the difference between the measured and simulate PUL resistance of the line.

The error function for the optimization process is defined as a root mean square difference:

$$F(\mathbf{x}) = \sqrt{\frac{\sum_{i=1}^{N}\left(\frac{R_{fit}(\mathbf{x},f_i)-R(f_i)}{R(f_i)}\right)^2}{N}} \tag{6}$$

where $\mathbf{x}$ is the set of the roughness parameters of the models, f is the frequency, N is the number of the frequency samples, and R_{fit} is the PUL resistance of the model. In (6), in the case of the differential pair, the PUL parameters are modal and relate to the common or differential mode. And $\mathbf{x}$ can be different when different roughness models are used, like in Huray model, $\mathbf{x}$ are nodule radius and surface ratio.

The constraints of the optimized roughness levels can be set based on the preliminary knowledge of the surface roughness of the board. For example, it can be assumed that the drum side of the conductors needs to be smoother than the matte side. If no information is available, the optimization range needs to be large enough to cover all expected foil roughness levels.

The optimization was performed using the optimization toolbox in Matlab. At each iteration, the Matlab script instructed the 2-D solver (Q2D) to simulate the geometry with current roughness values determined by the optimization routine.

III. Validation

A. Validation using Measurement Data

To validate the method proposed in section II, a testing vehicle is fabricated [10]. The cross-section of the coupled

stripline is shown in Fig. 2, and the corresponding geometrical parameters are listed in table I. Optical microscopy is performed to obtain the profile of rough conductors, as shown in Fig. 3. Using the roughness profile extraction tool [14], it is found that the root mean square (RMS) roughness levels for the signal trace and the reference planes are 0.41 μm and 0.47 μm, respectively.

Following the process introduced in section II, the relative permittivity and loss tangent of the dielectric material is extracted, as shown in Fig. 4. The variations below 4 GHz is caused by the measurement and simulation errors, as discussed in [10].

The roughness setting in Q2D is tuned to reconstruct the surface roughness level using the method presented in section II. Huray model was chosen to model the surface roughness in the 2D simulator. Huray model is characterized by the following parameters: nodule radius of the spheres a and the Hall-Huray surface ratio SR:

$$SR = \frac{4\pi N a^2}{A_{smooth}} \tag{7}$$

where N is the number of spheres within the tile of area A_{smooth}. The value of SR quantifies the distribution density of spheres.

There are two assumptions made here to determine the variables to be tuned in the optimization script. Firstly, since the optical microscopy results show that the roughness levels of signal trace and ground plane are comparable, it is assumed that all the conductor surfaces share the same roughness level. So only one set of roughness setting is needed. Secondly, it is assumed that two adjacent spheres are placed right next to each other on the smooth plane, as shown in Fig. 5. In this way, the value of A_{smooth} of one periodic unit can be calculated as $(2a)^2$, and $N = 1$. Thus, according to Eq. 7, the value of SR is fixed at π. So, there is only one parameter under optimization in this example, which is the radius of the spheres. The optimization range of a is from 0 to 1 mm, which is large enough to cover the roughness level of all common roughness profiles.

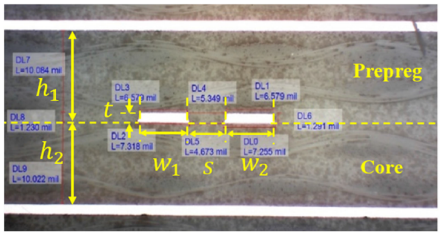

Fig. 2: Cross-section of the stripline under test.

TABLE I: Geometrical parameters of the stripline

Parameters	W_1	W_2	s	h_1	h_2	t
Value (mil)	6.58	6.58	5.30	10.05	10.05	1.23

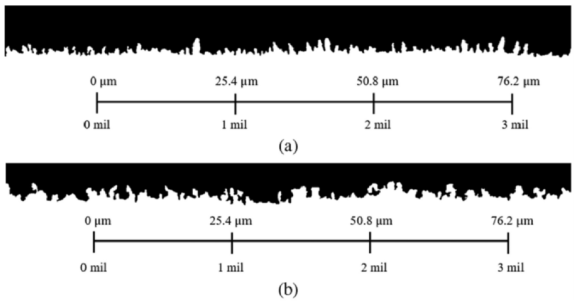

Fig. 3: Optical photo of (a) ground and (b) trace conductors.

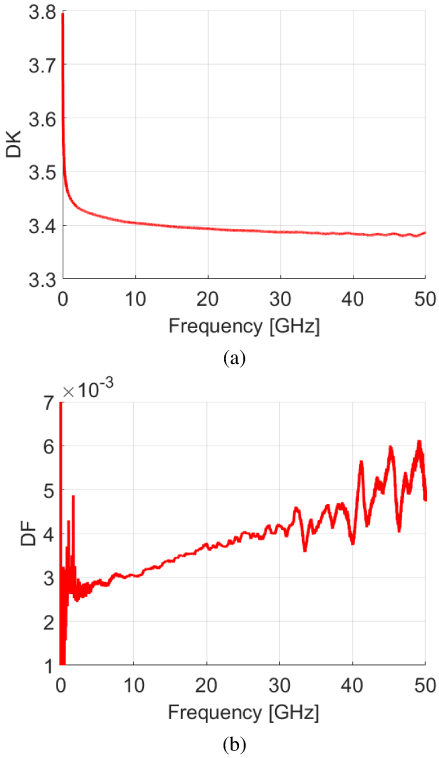

Fig. 4: Extracted (a): relative permittivity; (b): loss tangent of the test board.

The value of the PUL resistance R_{dd} at ten uniformly distributed frequency points from 1 GHz to 28 GHz serves as the target of optimization, where the subscript dd represents the differential mode. The values of R_{dd} at lower and higher frequencies are not used as the accuracy of the loss tangent extraction at those frequencies is poor as can be seen from Fig. 4b [15] [16].

The $fminbnd$ function implemented in the Matlab is used to optimize the nodule radius a within the constraint so that the value of the error function defined in (6) is minimized. The iteration will not stop until the number of iterations exceeded the predefined threshold or the error function converges. In this example, 18 iteration were needed for the error function to converge to 0.0013. The change of the error function

during the optimization process is shown in Fig. 6. The total optimization time was 16 minutes.

The optimized value of the PUL R for the differential mode is shown in Fig. 7 in comparison to the measured PUL resistance calculated according to (5). It is found that the optimization result correlates well with the measurement not only at the middle-frequency range but also at the higher frequencies, i.e. outside the range used in optimization. Further, the S-parameter can be calculated using the optimized PUL R together with the simulated PUL LGC. The comparison between the measured and calculated S_{21} is shown in Fig. 8. The final optimization result of nodule radius a is 0.43 um, which is very close to the RMS roughness levels obtained from optical microscopy. Thus, it is verified that using the measured S-parameter and cross-section information, the roughness level of conductors can be extracted accurately.

B. Validation using 2-D Simulation Data

Unfortunately, a suitable PCB with significantly different matte/drum side roughness was not available, and the ability of the method to extract non-uniform roughness was validated by simulation.

The simulation model shown in Fig. 9 is used. The corresponding geometrical parameters are listed in table II. The sphere radii on the drum and matte sides are set as 0.5 μm and 2 μm, respectively. The value of the simulated R_{dd} at ten frequency points uniformly distributed from 1 GHz to 50 GHz serves as the target.

TABLE II: Geometrical parameters of the stripline

Parameters	w	s	h_1	h_2	t
Value (mil)	7.32	2	5	10	1.3

In the optimization routine, the sphere radii of the upper and lower portions of the stripline are tuned using the pattern search algorithm implemented in Matlab until the fitted differential PUL resistance agrees with the target. The value of SR remains fixed at π. The optimization ranges of the two radii and the error function are the same as the example shown in section III-A. The change of relative error during the optimization is shown in Fig. 10. With more variables under optimization, it takes more iterations for the error function to converge. In this example, the optimization takes 1 hour 20 minutes in total and required 40 iterations.

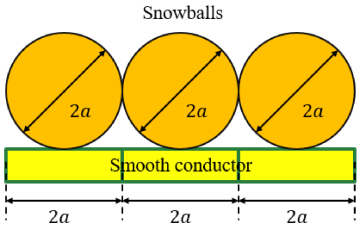

Fig. 5: Spheres are placed on top of smooth conductor and right next to each other.

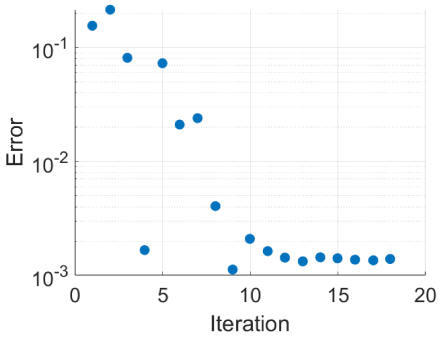

Fig. 6: Change of the error function during optimization.

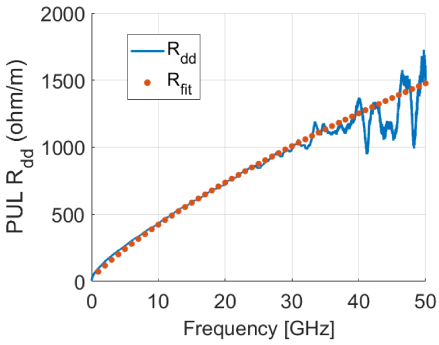

Fig. 7: Comparison between the target and optimized PUL resistance results.

In the end, the optimized roughness levels are 0.49 μm and 2.01 μm for the drum side and matte side respectively, which correlates well with the original settings in Fig. 9. The modal PUL resistances calculated after the optimization agree well with the target values, as shown in Fig, 11. In this way, it is demonstrated that the proposed method can extract roughness correctly for boards with non-equal roughness.

C. Validation using 3-D Simulation

The results in section III-B are obtained under the idealized conditions when the same model was used to generate the

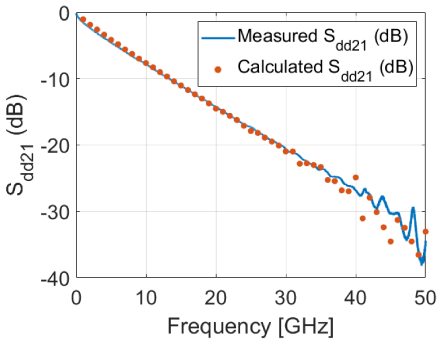

Fig. 8: Comparison between the measured and calculated S_{dd21}.

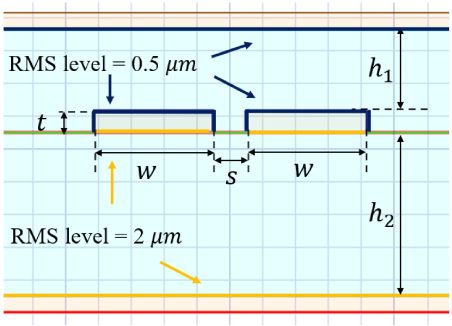

Fig. 9: Cross-section of the coupled stripline. Surfaces in blue are the drum side, and surfaces in yellow are the matte side.

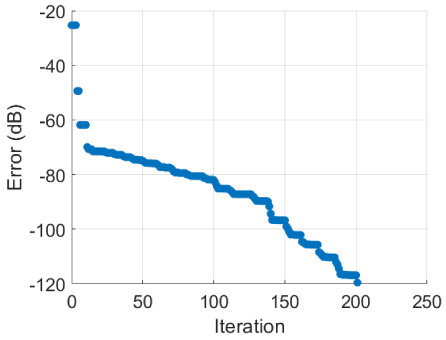

Fig. 10: Change of the error function during optimization.

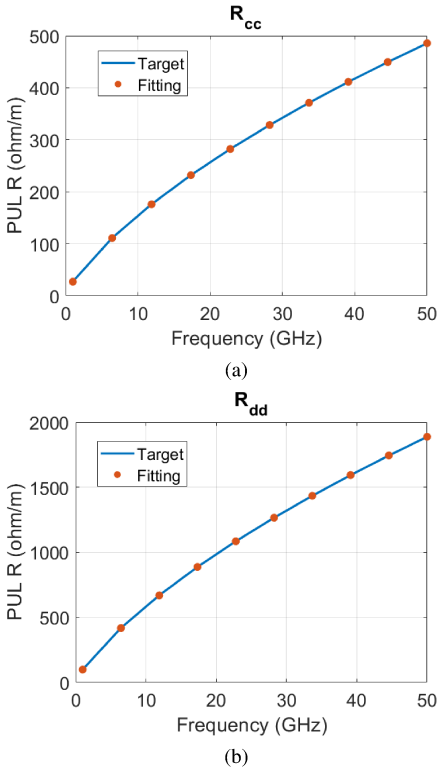

Fig. 11: Comparison between target and optimization result. (a): Common mode; (b): Differential mode.

reference values and during the optimization. This eventually led to negligible optimization errors. To validate the proposed method further, a 3D model of a simple two conductor transmission line is built in CST, as shown in Fig. 12 (this simplification was used because a more realistic stripline structure with geometrical roughness would result in a very large mesh cell count). Both top and bottom conductors are cooper, and the dielectric layer in the middle is vacuum. In this way, the contribution of α_{diel} is eliminated. Hemispheres with radii of 1 μm and 2 μm are added to the top and bottom conductors, respectively. Two side walls are set as the perfect magnetic conductor (PMC) to enforce transverse electromagnetic (TEM) wave.

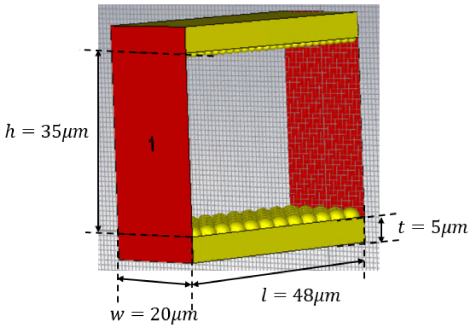

Fig. 12: 3D model of the transmission line with rough surface.

Next, the corresponding Q2D simulation model is created, as shown in Fig. 13, and optimized. The width of the two conductors is large enough to imitate the PMC boundary in the CST model. The optimization script used here is the same as the one described in section III-B. The roughness levels of two conductors in the Q2D model are continuously optimized. The change of the error function during the optimization is shown in Fig. 14. The final optimization results of hemisphere radii are 0.95 μm and 2.06 μm for the upper and lower conductor, which is close to the original settings in 3D model. The comparison of target and fitted results is shown in Fig. 15.

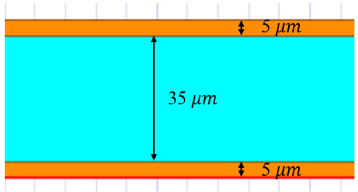

Fig. 13: Q2D model under optimization. The width of the conductor is 1000 μm.

IV. Conclusion

The traditional roughness modeling process requires cutting the test board and measuring the roughness of the sample through optical microscopy or SEM. To avoid such a process, a new methodology is presented in this paper. The roughness

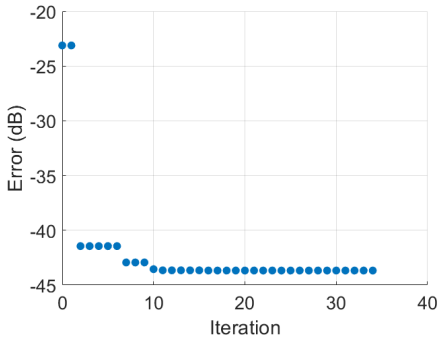

Fig. 14: Change of the error function during optimization.

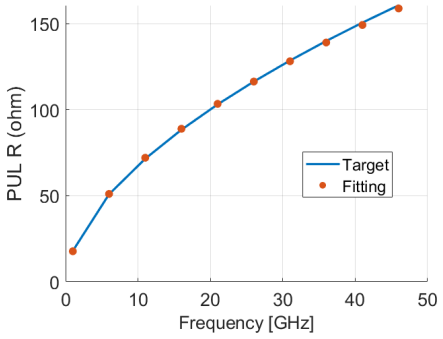

Fig. 15: Comparison between the target and optimization result.

level of cooper foil can be extracted iteratively using a 2D solver from the measured S-parameter and the nominal cross-sectional information of the board.

Compared with previous modeling approaches, the proposed method will not damage the test board and does not require microscopic measurement. The method has been validated on the lines with uniform roughness in an experiment and on the lines with non-uniform roughness in simulation. More validation will be provided in the future using measurement data of the routing striplines.

V. Acknowledgment

This work is supported in part by the National Science Foundation under Grant No. IIP-1916535.

References

[1] Guo, Y., Chen, B., Sun, X., Ye, X., Hsu, J., & Fan, J. (2019, June). Study of TDR impedance for better analysis to measurement correlation. In 2019 Joint International Symposium on Electromagnetic Compatibility, Sapporo and Asia-Pacific International Symposium on Electromagnetic Compatibility (EMC Sapporo/APEMC) (pp. 88-91). IEEE.

[2] Guo, Y., Kim, D., He, J., Yong, S., Liu, Y., Pu, B., & Fan, J. (2021, July). The Simulated TDR Impedance In PCB Material Characterization. In 2021 IEEE International Joint EMC/SI/PI and EMC Europe Symposium (pp. 831-834). IEEE.

[3] Sun, X., Guo, Y., Sun, Y., Song, K., Ye, L., Ye, X., & Fan, J. (2019, July). Causality analyzing for transmission line with surface roughness. In 2019 IEEE International Symposium on Electromagnetic Compatibility, Signal & Power Integrity (EMC+ SIPI) (pp. 516-521). IEEE.

[4] Huray, P. G., Oluwafemi, O., Loyer, J., Bogatin, E., & Ye, X. (2010). Impact of copper surface texture on loss: A model that works. DesignCon 2010, 1, 462-483.

[5] Yong, S., Khilkevich, V., Liu, Y., He, R., Guo, Y., Gao, H., & Drewniak, J. (2020, July). A Cross-sectional Profile Based Model for Stripline Conductor Surface Roughness. In 2020 IEEE International Symposium on Electromagnetic Compatibility & Signal/Power Integrity (EMCSI) (pp. 334-339). IEEE.

[6] Hammerstad, E., & Jensen, O. (1980, May). Accurate models for microstrip computer-aided design. In 1980 IEEE MTT-S International Microwave Symposium Digest (pp. 407-409). IEEE.

[7] Hall, S., Pytel, S. G., Huray, P. G., Hua, D., Moonshiram, A., Brist, G. A., & Sijercic, E. (2007). Multigigahertz causal transmission line modeling methodology using a 3-D hemispherical surface roughness approach. IEEE Transactions on Microwave Theory and Techniques, 55(12), 2614-2624.

[8] Jin, S., Chen, B., Fang, X., Gao, H., Ye, X., & Fan, J. (2017). Improved "Root-Omega" method for transmission-line-based material property extraction for multilayer PCBs. IEEE Transactions on Electromagnetic Compatibility, 59(4), 1356-1367.

[9] Yong, S., Liu, Y., Gao, H., Chen, B., De, S., Hinaga, S., & Khilkevich, V. (2018, July). Dielectric dissipation factor (DF) extraction based on differential measurements and 2-D cross-sectional analysis. In 2018 IEEE Symposium on Electromagnetic Compatibility, Signal Integrity and Power Integrity (EMC, SI & PI) (pp. 217-222). IEEE.

[10] Yong, S., Khilkevich, V., Liu, Y., Gao, H., Hinaga, S., De, S., & Drewniak, J. (2020). Dielectric loss tangent extraction using modal measurements and 2-D cross-sectional analysis for multilayer PCBs. IEEE Transactions on Electromagnetic Compatibility, 62(4), 1278-1292.

[11] Chen, B., Ye, X., Samaras, B., & Fan, J. (2015, May). A novel de-embedding method suitable for transmission-line measurement. In 2015 Asia-Pacific Symposium on Electromagnetic Compatibility (APEMC) (pp. 1-4). IEEE.

[12] Chen, B., He, J., Guo, Y., Pan, S., Ye, X., & Fan, J. (2019). Multi-Ports ($[2^n)$ 2×-Thru De-Embedding: Theory, Validation, and Mode Conversion Characterization. IEEE Transactions on Electromagnetic Compatibility, 61(4), 1261-1270.

[13] Chen, B., He, J., Sun, X., Guo, Y., Jin, S., Ye, X., & Fan, J. (2018, July). Differential S-parameter de-embedding for 8-port network. In 2018 IEEE Symposium on Electromagnetic Compatibility, Signal Integrity and Power Integrity (EMC, SI & PI) (pp. 52-56). IEEE.

[14] De, S., Gafarov, A., Koledintseva, M. Y., Stanley, R. J., Drewniak, J. L., & Hinaga, S. (2012, August). Semi-automatic copper foil surface roughness detection from PCB microsection images. In 2012 IEEE International Symposium on Electromagnetic Compatibility (pp. 132-137). IEEE.

[15] Liu, Y., Yong, S., Gao, H., Hinaga, S., Padilla, D., Yanagawa, D., & Khilkevich, V. (2020). S-Parameter De-Embedding Error Estimation Based on the Statistical Circuit Models of Fixtures. IEEE Transactions on Electromagnetic Compatibility, 62(4), 1459-1467.

[16] Yong, S., Liu, Y., Gao, H., Hinaga, S., De, S., Padilla, D., & Khilkevich, V. (2019, July). A practical de-embedding error analysis method based on statistical circuit models of fixtures. In 2019 IEEE International Symposium on Electromagnetic Compatibility, Signal & Power Integrity (EMC+ SIPI) (pp. 45-50). IEEE.